

Mutant p53^{R175H} upregulates Twist1 expression and promotes epithelial–mesenchymal transition in immortalized prostate cells

I Kogan-Sakin^{1,7}, Y Tabach^{2,7}, Y Buganim¹, A Molchadsky¹, H Solomon¹, S Madar¹, I Kamer¹, P Stambolsky¹, A Shelly¹, N Goldfinger¹, S Valsesia-Wittmann³, A Puisieux³, A Zundelich⁴, EN Gal-Yam⁴, C Avivi⁵, I Barshack⁵, M Brait⁶, D Sidransky⁶, E Domany² and V Rotter^{*,1}

A mutation within one allele of the *p53* tumor suppressor gene can inactivate the remaining wild-type allele in a dominant-negative manner and in some cases can exert an additional oncogenic activity, known as mutant p53 ‘gain of function’ (GOF). To study the role of p53 mutations in prostate cancer and to discriminate between the dominant-negative effect and the GOF activity of mutant p53, we measured, using microarrays, the expression profiles of three immortalized prostate epithelial cultures expressing wild-type, inactivated p53 or mutated p53. Analysis of these gene expression profiles showed that both inactivated p53 and p53^{R175H} mutant expression resulted in the upregulation of cell cycle progression genes. A second group, which was upregulated exclusively by mutant p53^{R175H}, was predominantly enriched in developmental genes. This group of genes included the Twist1, a regulator of metastasis and epithelial–mesenchymal transition (EMT). Twist1 levels were also elevated in metastatic prostate cancer-derived cell line DU145, in immortalized lung fibroblasts and in a subset of lung cancer samples, all in a mutant p53-dependent manner. p53^{R175H} mutant bearing immortalized epithelial cells showed typical features of EMT, such as higher expression of mesenchymal markers, lower expression of epithelial markers and enhanced invasive properties *in vitro*. The mechanism by which p53^{R175H} mutant induces Twist1 expression involves alleviation of the epigenetic repression. Our data suggest that Twist1 expression might be upregulated following p53 mutation in cancer cells.

Cell Death and Differentiation (2011) 18, 271–281; doi:10.1038/cdd.2010.94; published online 6 August 2010

Wild-type p53 (wt-p53) is a transcription factor that promotes cell cycle arrest, DNA repair, cellular senescence and apoptosis^{1,2} in response to stress stimuli. About 50% of human cancers have lost functional p53 mostly because of the mutations at the DNA-binding domain of p53.³ p53 mutants (mutp53) are being overexpressed and accumulated to very high levels in cancer cells;⁴ however, they are unable to recognize wt-p53 DNA-binding sites causing a loss of p53 tumor suppressor function. Furthermore, mutp53 acts as a dominant negative through hetero-oligomerization, with wt-p53 preventing its tumor suppressor activity.⁵ In addition, the most commonly occurring p53 core mutants display a gain of oncogenic function (GOF)⁴ actively promoting tumor progression. One of the major mechanisms underlying mutp53 GOF is its ability to regulate a large number of specific target genes.⁶ Although the idea of an oncogenic activity of mutp53 is widely acknowledged, the specific mechanisms underlying it remain to be fully elucidated.

Although prostate cancer is the most commonly diagnosed type of cancer in men, so far no cure is available for patients with advanced disease. In prostate cancer, mutations in the *p53* tumor suppressor gene are usually associated with poor prognosis. The reported frequency of p53 alterations in primary prostate cancer varies between 0 and 80%.⁷ Nevertheless, it is widely accepted that p53 mutations are common in advanced prostate cancer and correlate with metastasis and recurrence.⁸

One major drawback in investigating prostate cancer is the fact that commonly used prostate carcinoma cell lines are originated from metastatic lesions and contain multiple genetic alterations. On such a background, it is difficult to investigate a specific tumor suppressor or an oncogene with respect to cancerous processes. To be able to evaluate the authentic role of p53 in prostate carcinogenesis, we assessed the effect of p53 mutation in EP156T-immortalized prostate epithelial cells.⁹ Using this immortalized model, we could manipulate the cells in a controlled way and investigate

¹Department of Molecular Cell Biology, Weizmann Institute of Science, Rehovot, Israel; ²Department of Physics of Complex Systems, Weizmann Institute of Science, Rehovot, Israel; ³Inserm, U590, Lyon, France; ⁴Cancer Research Center, The Chaim Sheba Medical Center, Tel-Hashomer, Israel; ⁵Department of Pathology, The Chaim Sheba Medical Center, Tel-Hashomer, Israel and ⁶Department of Otolaryngology-Head and Neck Surgery, Johns Hopkins University School of Medicine, Baltimore, MD, USA

*Corresponding author: V Rotter, Department of Molecular Cell Biology, Weizmann Institute of Science, Rehovot 76100, Israel.

Tel: + 972-8-9344070; Fax: + 972-8-9465265; E-mail: varda.rotter@weizmann.ac.il

⁷Both these authors contributed equally to this work.

Keywords: p53; Twist1; prostate

Abbreviations: GOF, gain of oncogenic function; wt-p53, wild-type p53; mutp53, mutant p53; EMT, epithelial–mesenchymal transition; Coni, short hairpin control; H3K27me3, trimethylation of histone H3 at lysine 27; ChIP, chromatin immunoprecipitation

Received 17.12.09; revised 21.5.10; accepted 31.5.10; Edited by KH Vousden; published online 06.8.10

individual lines with specific genetic alterations. The proliferative behavior of immortalized cells expressing either wt, inactivated or mutated p53 was analyzed, and genomic profiling was performed. We identified cell-cycle-associated M-phase genes upregulated when p53 is inactivated or mutated, suggesting that mutp53 exerts a dominant-negative inactivation of wt-p53, which accelerates cell cycle progression. Furthermore, we found a unique group of genes implicated in both development and cancer progression, whose expression was increased only in cells harboring mutp53, suggesting a GOF activity of mutp53. We focused on elucidating the regulation of one gene from this list, the Twist1, which is an important regulator of epithelial–mesenchymal transition (EMT). The increase in Twist1 expression was correlated with characteristic features of EMT observed in mutp53-expressing cells. Altogether, our data suggest that mutp53 supports malignancy by accelerating cellular proliferation through a dominant-negative mechanism, and by inducing the EMT process through its GOF activity.

Results

Inactivation of wt-p53 in EP156T cells by GSE56 or p53^{R175H} mutant overexpression confers cells with significant proliferation advantages. hTERT-immortalized prostate epithelial EP156T cells retained intact wt-p53 activity.⁹ The p53^{R175H} mutation is commonly found in cancer cells including prostate cancer,¹⁰ and it is known to confer an oncogenic GOF activity on a background of wt-p53.⁴ To investigate the effect of p53 mutation, EP156T cells (at passage 25) were infected with a recombinant retrovirus encoding with either p53^{R175H} mutant (M cells), dominant-negative p53 peptide GSE56 (G cells) or control vector (C cells) (Figure 1). The GSE56 served as a control for mutp53 GOF. To obtain a complete picture, we investigated the effect of the above alterations on the development of oncogenic features at several points along the immortalization process. A number indicating the approximate number of passages (± 3) at which the specific sample was attached to sample labels was also investigated.

C40, G40 and M40 cells were treated for 6 h and for 16 h with DNA-damaging agent doxorubicin. Then, p53 protein stabilization and mRNA levels of p53 target genes were examined to test whether wt-p53 activity was compromised in GSE56- and mutp53-expressing cells. p53 protein stabilization and efficient upregulation in the expression of p21^{waf1} and PUMA mRNA upon doxorubicin were observed in C40 cells (Figure 1a). In G40 and M40 cells, p53 protein levels were very high both in the treated and in the non-treated samples in agreement with the expected accumulation of inactive wt-p53 upon infection with GSE56 in G cells and accumulation of mutp53 upon p53^{R175H} overexpression in M cells. In accordance with this, induction of p21^{waf1} and PUMA transcription was strongly attenuated in both G40 and M40 cells at the 6-h time point. Notably, in M40 cells there was an upregulation in the mRNA levels of p21^{waf1} and PUMA after 16 h of treatment, although the mRNA levels were still significantly lower than that in the C40 cells. Thus, mutp53 overexpression only partially interferes with wt-p53

function in response to DNA damage. To evaluate whether the partial dominant-negative effect detected in EP156T cells can be observed in an additional cellular system, we used hTERT-immortalized primary lung fibroblasts WI-38¹¹ infected with GSE56 or p53^{R175H}. A similar pattern was evident (Figure 1b) confirming partial wt-p53 inactivation by mutp53.

To evaluate the effect of p53 inactivation on cell growth, mean doubling time along 400 days *in vitro* was calculated for each culture. This analysis indicated that G and M cells were proliferating more rapidly than C cells (Figure 1c). To reinforce this observation, we compared colony-forming efficiencies of the three cell lines. C70, G70 and M70 cells were seeded at clonal density and the number of colonies was counted after 2 weeks of incubation. Both G70 and M70 lines exhibited a higher colony-forming efficiency, as shown by their colonies number and size distribution when compared with C70 cells, which barely induced any colonies (Figure 1d). These data suggest that the increase in the proliferation rate in G and M lines results mostly from p53 inactivation rather than a specific GOF activity.

Dominant-negative inactivation of wt-p53 versus GOF of p53^{R175H} effects on gene expression.

Next, we wished to assess the effect of mutp53 on gene expression. Samples of each of the three lines were subjected to genomic profiling by cDNA microarray in 10-passage intervals (Figure 2a). First, we evaluated the dominant-negative effect of wt-p53 inactivation. To this end, GSE56 upregulated genes were determined. This analysis yielded a list of 303 upregulated genes (Supplementary Table S1) that were also upregulated, although to a slightly lower extent in the M line. Functional annotation analysis revealed that this list was enriched with genes that belong to the 'cell cycle phase' (Supplementary Table S2). Their levels in the different samples are illustrated in a 'heat map' (Figure 2b) showing that the onset of this 'cell cycle phase' gene expression in both G and M lines occurs at passage 40, which is 30 passages earlier than that in the C line. We validated this expression pattern by measuring the mRNA levels of *AURKA*, *BIRC5* and *CDC20*, as representative genes, using quantitative real-time PCR (QRT-PCR) (Figure 2c, upper panel). Western blotting for *CDC20* was used for protein confirmation (Figure 2c, lower panel). Notably, the increase in cell proliferation rate and the higher colony-forming efficiency of G and M lines compared with the C line (Figure 1b and c) are consistent with higher levels of 'cell cycle phase' gene expression.

To evaluate the mutp53 GOF effect, we isolated a mutp53-specific gene expression profile (Supplementary Table S3) as described in the Materials and methods section. The most significant enrichment was found for 'multicellular organismal development' (Figure 2b). This pattern was validated by QRT-PCR for *GREM1*, *SLITRK5* and *Twist1* as representatives (Figure 2c, middle panel). Western blotting analysis for *SLITRK5* and *Twist1* confirmed QRT-PCR observations (Figure 2c, lower panel). Importantly, knocking down endogenous wt-p53 by shp53 (Supplementary Figure S1A) did not induce the expression of *GREM1*, *SLITRK5* or *Twist1* as was in the case of mutp53 overexpression (Supplementary Figure S1B), supporting the notion that the induction of these genes in the M line was due to mutp53 GOF mechanism and not

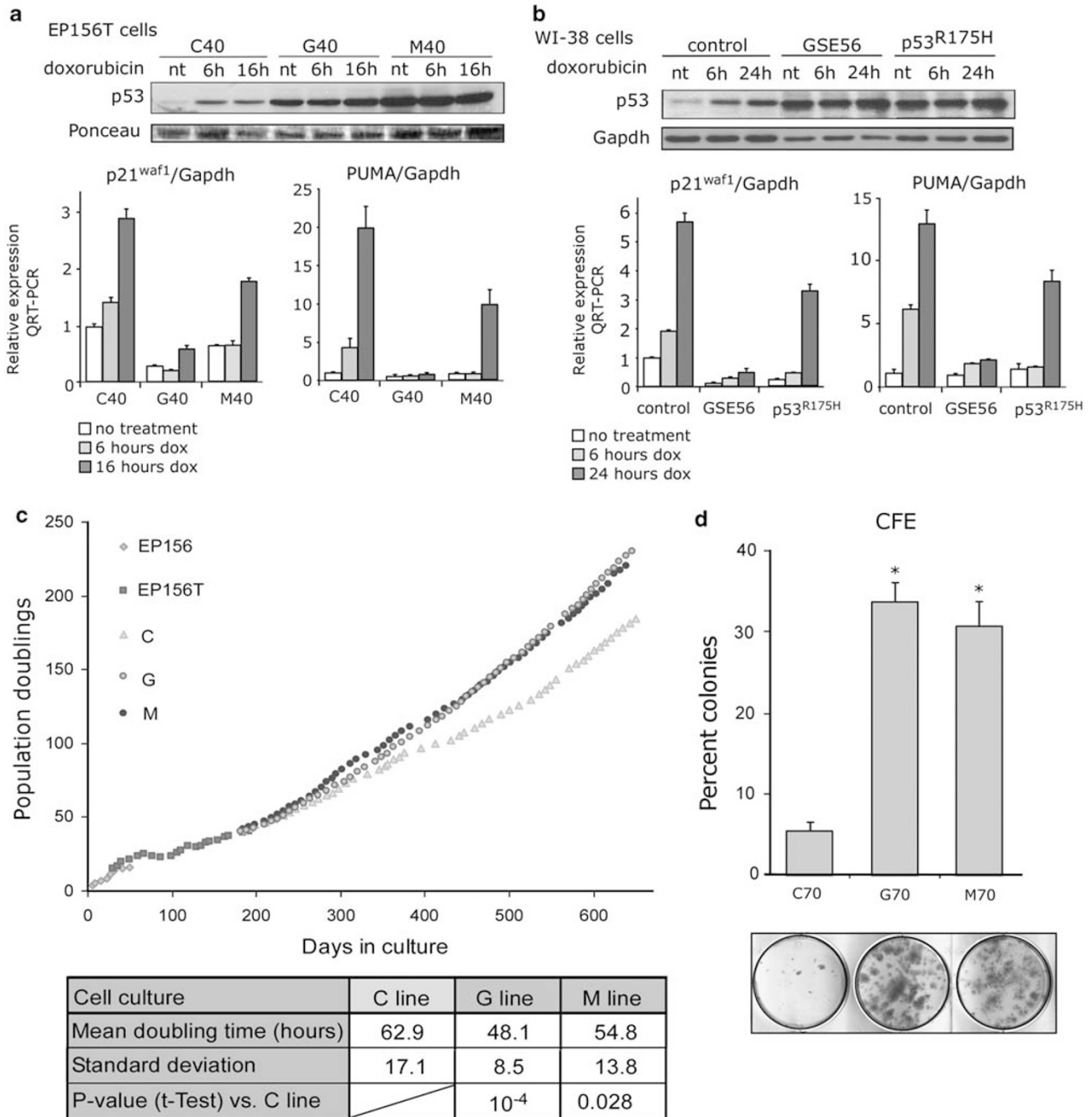


Figure 1 Inactivation of wt-p53 function in EP156T cells through GSE56 or p53^{R175H} mutant overexpression. (a) C40, G40 and M40 cells were treated with doxorubicin (0.2 μ g/ml) and p53 protein levels were tested by western blotting. Ponceau staining and GAPDH were used as loading controls. mRNA levels of p21^{waf1} and PUMA were tested by QRT-PCR. (b) Same experiment as in (a) was performed in hTERT-immortalized WI-38 cells. (c) Proliferation plot of C, G and M cells. Cell growth rate parameters are presented in the table at the bottom of the graph. *P*-values calculated by *t*-test for G and M lines compared with C line represent statistically significant differences in cell growth of C line and those of G and M lines. (d) Colony formation efficiency was tested for C, G and M cells. Three hundred cells/well were seeded in a six-well plate and incubated for 2 weeks. Then, the colonies were stained with crystal violet and scored. Asterisks depict statistically significant differences between the control cells (C line) and the GSE56 (G) or p53^{R175H} (M) mutant-infected cells (**P* < 0.0005)

through wt-p53 inactivation. Altogether, our results show a specific expression profile for the dominant-negative effect, which is correlated with proliferation and a distinct expression profile specific for mutp53 GOF, which is connected to development.

Mutp53 specifically elevates Twist1 expression. Genes that normally function in developmental processes are often deregulated in cancer. Twist1 that appeared in our list of *mutp53* upregulated genes is involved in tumor metastasis through an induction of EMT.¹² In prostate cancer, strong

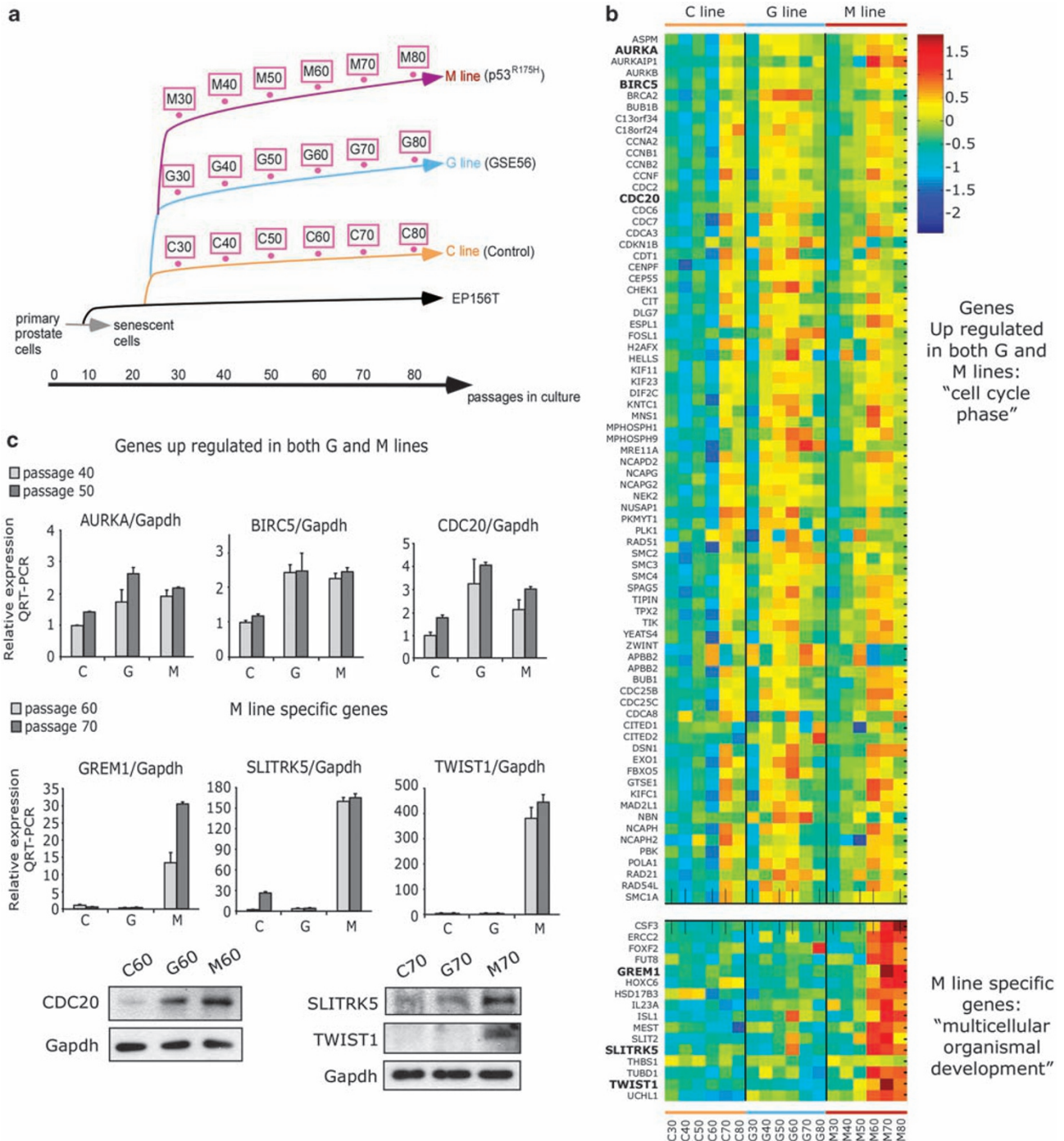


Figure 2 Genome-wide expression screen to identify changes following GSE56 and p53^{R175H} introduction into immortalized EP156T cells. **(a)** Schematic representation of the EP156T-derived C, G and M cultures. The points represent samples that were subjected to microarrays. **(b)** Heat map representation of Affymetrix data depicting the gene expression changes in cells differing in their p53 status. Only the most significant gene ontology groups are presented. **(c)** Validation of gene expression changes by QRT-PCR and western blotting

nuclear Twist1 staining correlates with high Gleason score and metastasis.^{13,14} Thus, we decided to investigate whether a molecular cross-talk exists between mutp53 and Twist1 expression in M cells. Interestingly, Twist1 upregulation was initially evident at passage 40, which is 15 passages after p53^{R175H} was introduced to the cells. To validate that Twist1

upregulation in M cells is specifically dependent on the expression of mutp53, p53^{R175H}-expressing cells were stably infected with shp53 (M60-p53i) and the levels of Twist1 were determined. Wt-p53-expressing cells (C60) were also infected with shp53 (C60-p53i) and were used as a control. Notably, immediately after the knock down, although mutp53

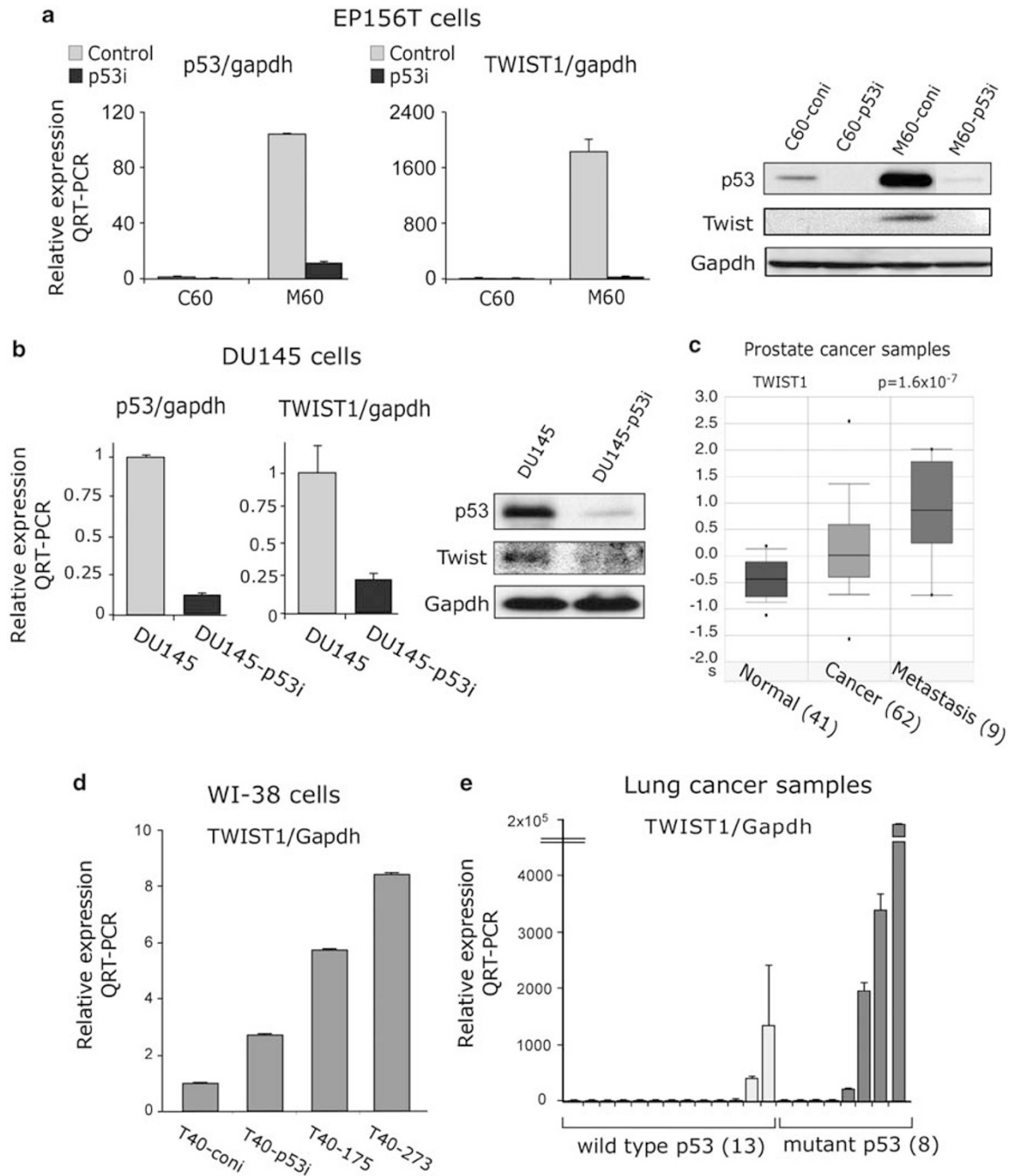


Figure 3 Mutant p53 upregulates Twist1 expression. (a) p53^{R175H}-bearing EP156T cells (M60) and the wt-p53 control cells (C60) were stably infected with shp53 (M60-p53i and C60-p53i, respectively) and the levels of p53 and Twist1 were determined by QRT-PCR and western blotting. GAPDH was used as a loading control. Wt-p53-bearing cells (C60) infected with shp53 (C60-p53i) were used as a control. (b) Endogenous mutant p53-bearing DU145 cells were stably infected with shp53 (DU145-p53i) and the levels of p53 and Twist1 were determined by QRT-PCR and Western blotting. GAPDH was used as a loading control. (c) An *in silico* comparison between normal prostate tissue, prostate carcinoma and metastatic prostate cancer using the 'ONCOMINE' microarray database shows a significant upregulation of Twist1 expression in metastasis. The indicated *P*-value is for Twist1 upregulation in metastasis as compared with localized prostate carcinoma. (d) Immortalized WI-38 cells from passage 40 stably infected with p53^{R175H} (T40-175) and p53^{R273H} (T40-273) mutants tested for Twist1 expression by QRT-PCR. Shp53 (T40-p53i) and empty vector (T40-coni) were used as controls. (e) mRNA levels of Twist1 were measured by QRT-PCR in 21 human lung cancer samples. p53 status of every sample is indicated on the axis

levels were about fourfold lower in cells infected with shp53 as compared with cells infected with control vector, the levels of Twist1 remained high (not shown). However, three passages after shp53 introduction, QRT-PCR and

western blotting indicated that Twist1 was efficiently down-regulated in M cells (Figure 3a). To examine whether Twist1 regulation by mutp53 is a general phenomenon, endogenous mutp53 carrying DU145 cells were stably infected with shp53

and Twist1 expression was tested. Figure 3b shows a decrease in Twist1 levels following mutp53 knockdown in DU145. Furthermore, to evaluate whether Twist1 mRNA levels were higher in clinical progression samples in prostate cancer, we performed an *in silico* comparative analysis by searching ONCOMINE microarray database. This analysis indicated that Twist1 mRNA levels were increased in metastatic prostate cancer samples as compared with normal and localized cancer samples (Figure 3c).

To test whether mutp53 may also induce Twist1 expression in additional cellular systems, we infected the immortalized WI-38 lung fibroblasts with either p53^{R175H} or p53^{R273H} mutants or with shp53 as a control for the loss of wt-p53 function. Both p53^{R175H} and p53^{R273H} mutants overexpression resulted in the upregulation of Twist1 mRNA in WI-38 cells (Figure 3d), further supporting our original observation that mutp53 elevates Twist1 mRNA expression levels.

Finally, we measured the expression levels of Twist1 in a subset of human lung cancer samples whose p53 status was predefined. Judged by QRT-PCR, it appears that a higher proportion of samples with mutp53 expressed high levels of *Twist1* gene (4/8) compared to samples with wt-p53 (2/13) (Figure 3e). Thus, mutp53 elevates Twist1 expression levels in prostate epithelial cells, prostate cancer cell line, fibroblasts and lung tumors by a specific GOF mechanism.

The prostate epithelial p53^{R175H}-expressing cells display characteristic features of EMT. As high Twist1 expression in tumors was shown to induce EMT,¹² it was important to evaluate whether mutp53-expressing cells, which also express high levels of Twist1, display characteristic features of EMT. To this end, we tested the mRNA levels of EMT markers in our immortalized cultures. As Figure 4a shows, M cells that highly express Twist1 indeed showed an increased level of EMT markers fibronectin1, MMP3 and MMP9. On the other hand, the levels of epithelial markers E-cadherin, desmoplakin, DSC3 and ΔNp63 were significantly reduced in M cells as compared with C and G cells (Figure 4a). Furthermore, immunofluorescent staining showed weaker intensity for E-cadherin and much stronger intensity for fibronectin1 in M cells as compared with C and G cells (Figure 4b). We further tested whether M cells also show more potent invasive capabilities. Indeed, M80 cells performed approximately two times better than C80 and G80 cells in an *in vitro* invasion assay (Figure 4c). Acquisition of invasive properties in tumors usually correlates with the loss of normal tissue architecture. As Twist1 is a known regulator of morphogenesis, we utilized a three-dimensional matrigel assay of glandular morphogenesis¹⁵ to compare C, G and M cells. In our previous study, EP156T as well as prostate primary epithelial cells seeded in Matrigel-coated wells, created three-dimensional spheroid structures resembling glandular buds and indicative of intact morphogenesis.⁹ When C80, G80 and M80 cells were seeded on the Matrigel, all three cultures were able to create spheroids that look very similar and closely resemble spheroids created by normal prostate epithelial cells (data not shown). This indicates normal pattern of morphogenesis in all three cultures. Overexpression of oncogenes often disrupts this normal morphogenesis process.¹⁶ To test whether there will be any

difference in glandular morphogenesis of EP156T cultures in the presence of oncogenic stimulation, we introduced the *H-Ras*^{V12} oncogene into C80, G80 and M80 cells, and then tested their ability to create spheroids. Figure 4d shows that while C80-Ras^{V12} and G80-Ras^{V12} formed well-ordered spheroids in three-dimensional cultures, M80-Ras^{V12} cells created unordered structures with extensions and multiple acini indicative of disruption of normal morphogenesis. Overexpression of H-Ras^{V12} was validated by western blotting (Figure 4d). Twist1 expression pattern was not altered by H-Ras^{V12}. Collectively, these data suggest that M cells display characteristic features of EMT, enhanced invasive properties *in vitro* and a defect in normal pattern of morphogenesis.

Twist1 activation by mutp53 is mediated through attenuation of epigenetic repression. Our next experiment aimed to elucidate the mechanism responsible for Twist1 upregulation in M cells. To test whether mutp53 induces transcriptional activation of Twist1 promoter, we first performed a reporter gene assay. A 1.3-kb DNA fragment upstream of the transcription start site of human *Twist1* gene fused to *luciferase* reporter gene was used. Reporter assays were performed in C60 and M60 cells infected with shp53 or with short hairpin control (con). As Figure 5a shows, Twist1 promoter reporter was activated to similar levels in all of the examined cell lines. p21^{waf1} promoter used as a control showed the highest levels of activity in wt-p53-expressing C60-coni cells as expected (Figure 5a). This implies that mutp53-mediated upregulation of Twist1 could be achieved through genomic modifications, which are not detected using artificial promoter.

Changes in epigenetic repression are involved in both the normal development and cancer.¹⁷ As Twist1 was not expressed in cultured prostate epithelial cells, we hypothesized that it could be silenced by an epigenetic mechanism and that mutp53 introduction disrupts this repression leading to Twist1 expression. To test this possibility, we treated the cells with DNA methylation inhibitor 5-azacytidine in combination with histone deacetylase inhibitor, trichostatin A. Figure 5b shows that this treatment induced a significant upregulation in Twist1 mRNA levels in C cells. Importantly, no effect was observed following the treatment in the M line, suggesting that epigenetic modifications have an important role in Twist1 upregulation by mutp53. To test whether the Twist1 promoter is less methylated in M cells, we performed methylated DNA immunoprecipitation. However, no significant difference in Twist1 promoter methylation was noticed comparing M and C cells (data not shown). Thus, increased Twist1 levels following 5-azacytidine and trichostatin A treatment might be through activation of other targets affecting Twist1 expression. To further unravel the mechanism of Twist1 activation in M cells, we re-evaluated our microarray expression data, searching for genes whose expression would show either direct or inverse correlation with Twist1 expression. We assumed that such genes might be functioning as mediators of epigenetic regulation of Twist1 expression. Interestingly, the *BMI-1* gene, a component of the polycomb repression complex involved in trimethylation of histone H3 at lysine 27 (H3K27me3), was one of the genes

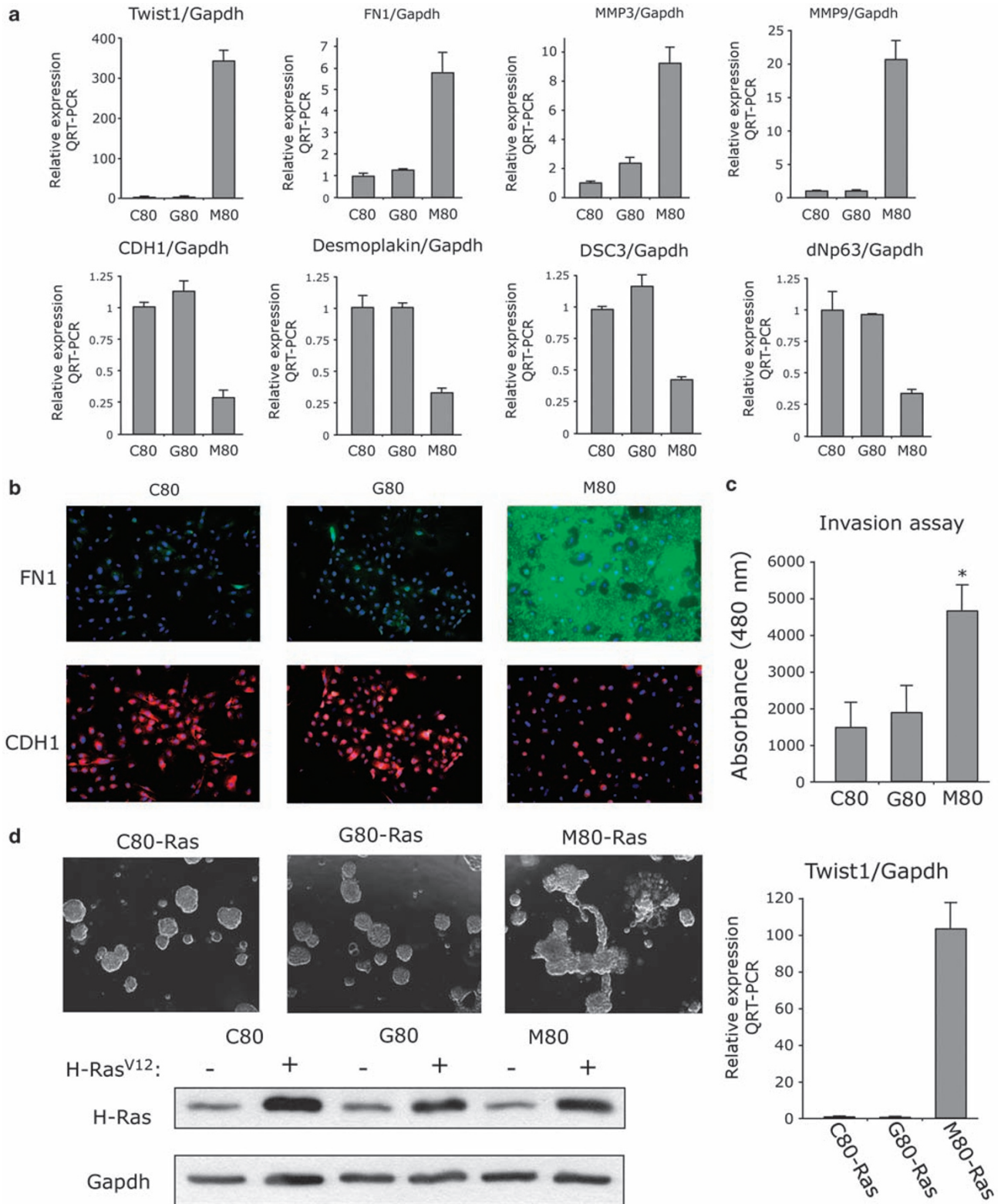


Figure 4 Mutant p53 induces EMT in immortalized prostate epithelial cells. (a) mRNA levels of Twist1, fibronectin1, MMP3, MMP9, E-cadherin, desmoplakin, DSC3 and dNp63 were analyzed by QRT-PCR in C80, G80 and M80 cells. (b) Immunofluorescent staining for E-cadherin and fibronectin1 in C80, G80 and M80 cells. (c) Invasion through matrigel towards 10% fetal calf serum by C80, G80 and M80 cells using transwells with 8- μ m pores. Asterisk depicts statistically significant difference in the number of invading cells between the control culture (C cells) and mutant p53-bearing culture (M cells). * $P=0.021$. (d) Following stable infection with H-Ras^{V12} cells were seeded for a three-dimensional morphogenesis assay. Formation of spheroids was examined and images were taken 10 days after seeding the cells using $\times 50$ magnification

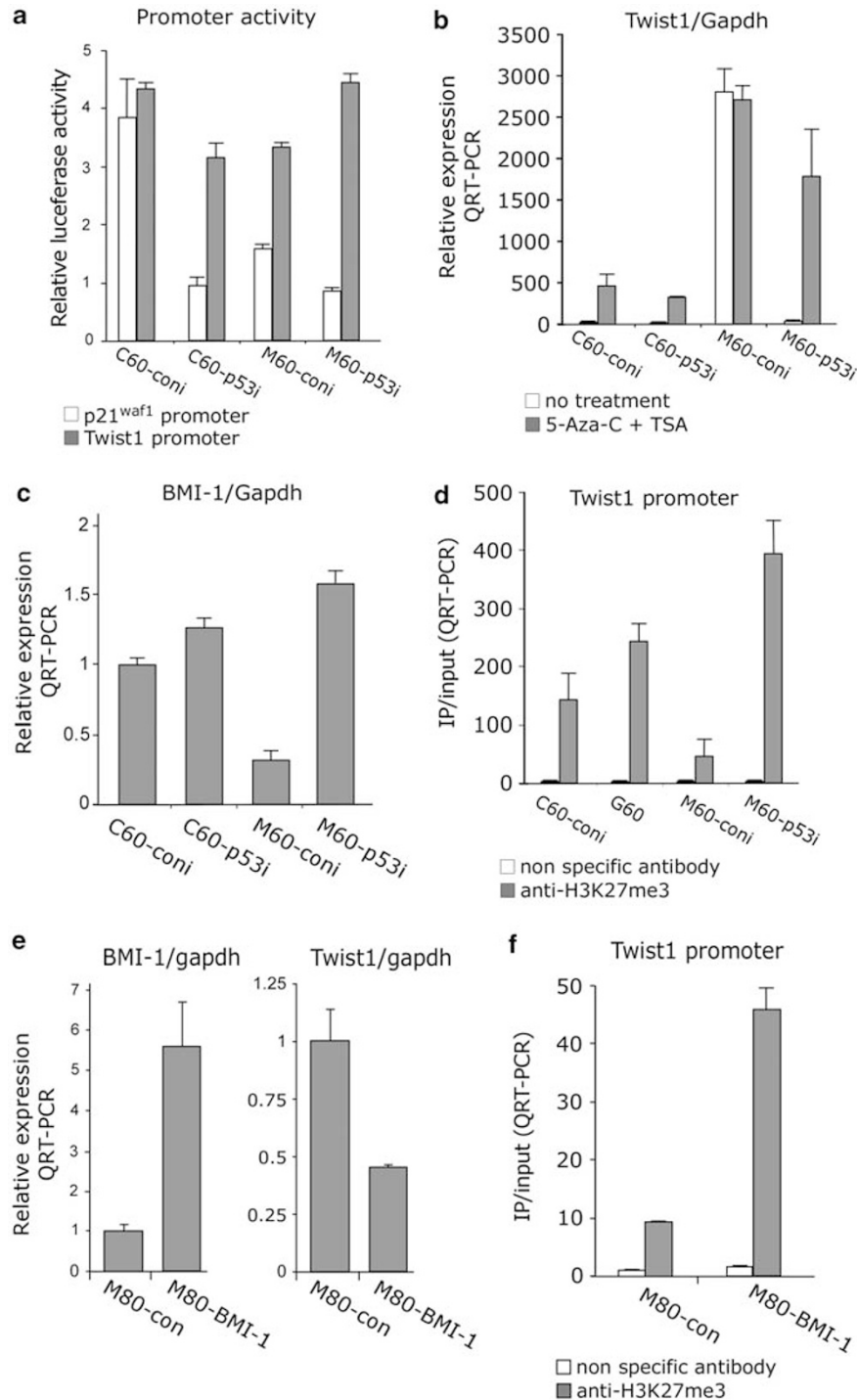


Figure 5 Twist1 upregulation by p53^{R175H} mutant is owing to reduction in BMI-1 expression and H3K27me3 on Twist1 promoter. (a) C60 and M60 cells stably infected with shp53 or control were transiently transfected with p21^{waf1} or Twist1 promoter-luciferase reporter. Reporter activity was determined 24 h later. Transfection efficiency was normalized on the basis of the activity of the co-transfected *Renilla* luciferase. (b) C60 and M60 cells stably infected with shp53 or control were treated with a combination of 5 μ M 5-azacytidine for 4 days and 500 nM trichostatin A for the last 12 h, and mRNA levels of Twist1 were evaluated by QRT-PCR. (c) mRNA levels of BMI-1 were determined in C60-coni, C60-p53i, M60-coni and M60-p53i by QRT-PCR. (d, f) ChIP was conducted on C60-coni, G60, M60-coni and M60-p53i cells (d) or on M80-con and M80-BMI-1 cells (f). Protein-DNA complexes were immunoprecipitated with an antibody against H3K27me3 or a nonspecific antibody (anti-TGF β R2). The amount of precipitated DNA was measured by QRT-PCR with specific primers directed against Twist1 promoter, and normalized to the input. (e) M80 cells were stably infected with either control vector (M80-con) or with BMI-1 expression plasmid (M80-BMI-1) and the levels of BMI-1 and Twist1 were determined by QRT-PCR

whose expression showed an inverse correlation to Twist1 expression. We validated mutp53-dependent expression pattern of BMI-1 by QRT-PCR and indeed found that BMI-1 was downregulated in M cells (Figure 5c). As BMI-1 is involved in the maintenance of H3K27me3 epigenetic repression mark, especially relevant for developmental genes,¹⁸ we examined the possibility of differential H3K27me3 levels in the Twist1 promoter of Twist1-expressing versus Twist1-non-expressing cells. Therefore, we performed chromatin immunoprecipitation (ChIP) using an antibody to H3K27me3 followed by QRT-PCR for Twist1 promoter region, 40-bp upstream to transcription start site in the different cell lines. Indeed, lower levels of H3K27me3 on Twist1 promoter in M cells were observed (Figure 5d). Importantly, there was a significant increase in H3K27me3 following knock down of p53^{R175H} by shRNA in M cells (Figure 5d). This is consistent with BMI-1 upregulation in the same sample (Figure 5c). Therefore, it was of interest to examine whether BMI-1 overexpression in M cells would directly methylate Twist1 promoter and reduce Twist1 levels. To explore this possibility, M80 cells were stably infected with BMI-1 (Figure 5e). QRT-PCR indicated that BMI-1 overexpression resulted in a reduction of Twist1 expression (Figure 5e). Furthermore, ChIP indicated that BMI-1 overexpression remarkably elevated the level of H3K27me3 on Twist1 promoter (Figure 5f). Thus, BMI-1 downmodulation in M cells is identified as a key factor for Twist1 induction by mutp53. Taken together, our results suggest that mutp53-dependent upregulation of Twist1 is mediated through a reduction of H3K27me3 repression mark on Twist1 promoter owing to BMI-1 downregulation by p53^{R175H}.

GOF of mutp53 was previously shown to be attributable to p63 inhibition by mutp53.^{19,20} Furthermore, p63 has an essential role in the biology of epithelial tissues.²¹ Therefore, we decided to test whether p63 inhibition by mutp53 can account for mutp53 GOF in Twist1 upregulation and EMT in EP156T cells. To this end, C60 cells were infected with shp63. p63 downregulation following shp63 infection was validated by QRT-PCR and western blotting (Supplementary Figure S2A). However, this treatment did not result in either BMI-1 downregulation or Twist1 induction (Supplementary Figure S2B). Thus, p63 inhibition most likely is not responsible for mutp53 GOF in the induction of Twist1 expression and EMT in EP156T cells.

Discussion

In this study, we aimed to differentiate between the dominant-negative inactivation of the wt-p53 by the mutp53 and mutp53 GOF activity. The data presented indicate that while dominant-negative inactivation of wt-p53 results in the upregulation of genes involved in cell cycle progression and cell growth, the GOF effect is reflected in the upregulation of development-associated genes and EMT phenotype. This phenotype is likely achieved by the upregulation of EMT-inducing transcription factor Twist1 by the p53^{R175H}. Although the GOF effect of mutp53 on proliferation and invasion was shown previously,²² this is the first report showing the connection between p53 mutation and EMT process, including a remarkable increase in Twist1 expression.

Our results suggest that both inactivation of p53 by GSE56 and p53^{R175H} mutant overexpression deregulate p53 pathway to induce the expression of genes involved in cell cycle progression. However, there was higher expression of cell cycle genes in cells with GSE56 than in cells with p53^{R175H}. This might indicate that GSE56 imposes a stronger dominant-negative effect on wt-p53 than p53^{R175H} does. This notion is supported by the results obtained following DNA damage (Figure 1a) showing higher expression of p53 target genes in M cells than in G cells.

The observation that shp53-bearing WI-38 cells express higher levels of Twist1 than wt-p53-bearing counterparts (Figure 3d) suggests that wt-p53 might inhibit Twist1. Notably, mutp53-expressing WI-38 cells showed even higher levels of Twist1 expression, indicating that mutp53 activates Twist1 expression in an independent manner and not through wt-p53 inactivation.

Several reports show mutp53 GOF, where mutp53 is able to upregulate gene expression through binding the promoters of specific genes.²³ Reporter gene assay including 1.3-kb Twist1 promoter indicated similar level of reporter activation in Twist1-expressing M cells and in Twist1-non-expressing cells, and we concluded that mutp53 regulates Twist1 expression by a different mechanism. Yet, it cannot be excluded that other than 1.3-kb upstream sequences might be important for the regulation of Twist1 expression by mutp53 in addition to epigenetic regulation.

The BMI-1 component of the polycomb repression complex was identified as a mutp53-repressed gene. Furthermore, reduced levels of H3K27me3 were found at the Twist1 promoter region in mutp53 cells. Overexpression of BMI-1 in mutp53 cells induced elevation of H3K27me3 in Twist1 promoter and a reduction of Twist1 expression was observed. Low BMI-1 expression levels in M cells appear controversial because BMI-1 is broadly accepted as an oncogene. Nevertheless, a recent report identified BMI-1 expression as a favorable prognostic factor in breast cancer patients.²⁴ An additional study reported that BMI-1 overexpression correlated with a good outcome in breast cancer and p53 mutation correlated with low BMI-1 levels.²⁵ These studies support our conclusion that mutp53 downregulates BMI-1 expression levels.

Prostate cancer at advanced stage, which is closely associated with p53 mutation, is virtually incurable. Our data suggest that mutp53 protein induces Twist1 expression in epithelial cells in which otherwise Twist1, a known inducer of EMT, is not detectable. Twist1 was previously suggested as a good candidate for targeted therapy of prostate cancer patients.¹⁴ Our findings further support this approach and suggest that targeting mutp53 may deplete Twist1 levels and reduce the invasiveness of cancer cells.

Materials and methods

Cell cultures. EP156T cells and WI-38 cells were maintained as described.^{9,11} The DU145 cells and the ecotropic retrovirus-producing (Phoenix) cells were obtained from the American Type Culture Collection (ATCC, Manassas, VA, USA) and cultured according to ATCC's instruction. The infection procedures using ecotropic Phoenix-packaging cells were described in Milyavsky *et al*.¹¹

Retroviral constructs. The pRetroSuper-p53 shRNA-Blast, the pRetroSuper-shmNOXA-Blast (control for shRNA) and the pBabe-H-Ras^{V12}-Hygro constructs were kindly provided by Dr. Doron Ginsberg (Bar-Ilan University, Ramat-Gan,

Israel). The PLXSN-GSE56-Neo and PLXSN-p53R175H-Neo vectors were generated in our laboratory by Dr Michael Milyavsky *et al.*¹¹ The retroviral BMI-1 overexpression construct pBabe-puro-BMI-1 was generously provided by Dr Goberdhan Dimri. The BMI-1 insert was subcloned from this vector into pBabe-Hygro. The p63 shRNA construct for total p63 knockdown (pSuper-Puro-totp63) was obtained from Dr Moshe Oren and then subcloned into the retroviral pRetroSuper-Hygro vector.

Western blotting analysis. For western blotting, total cell extracts were fractionated by gel electrophoresis and proteins were transferred to nitrocellulose membranes. The following primary antibodies were used: rabbit polyclonal anti-p53 (produced in our laboratory), anti-CDC-20 (sc-8358; Santa Cruz, Santa Cruz, CA, USA), anti-Twist (Twist2C1a, sc-81417; Santa Cruz), anti-p63 (4A4, sc-8431; Santa Cruz), anti-SLITRK5 (AB67309; Abcam, Cambridge, MA, USA) and anti-GAPDH (MAB374; Biotest); the protein-antibody complexes were detected by horseradish peroxidase-conjugated secondary antibodies followed by the ECL western blotting detection reagents (Amersham, Buckinghamshire, UK).

cDNA microarrays. cDNA microarrays were performed using the GeneChip Human Genome U133A 2.0 Array (Affymetrix, Santa Clara, CA, USA). The DNA for the microarrays was prepared according to the manufacturer's instructions.

Microarray data analysis. To evaluate the dominant-negative effect of wt-p53 inactivation, we compared the gene expression patterns of the G line with the control C line. We searched for genes that were at least 1.6-fold upregulated in the G line at each time point (i.e. C30–G30, C40–G40, etc.). To find genes that were stably upregulated in G cells, only the genes that were altered at least in three sequential time points were selected. This analysis yielded a list of 303 upregulated genes (Supplementary Table S1). These genes were upregulated to a slightly lower extent in the M line as well. The functional annotations of the 303 gene list were examined using 'gene ontology'.²⁶ Consequently, the gene ontology of the 'cell cycle phase' showed the most significant enrichment of 75 genes (P -value = 2.2×10^{-60}) as calculated by the DAVID database²⁷ (see Supplementary Table S2).

To evaluate the GOF effect, the gene expression patterns of the M line were compared with those of the control C line and only the genes that were at least 1.6-fold upregulated at three sequential time points were chosen for further analysis. From those genes we subtracted all genes that were also upregulated in the G line. The upregulation of the remaining 37 genes (Supplementary Table S3) in the M line is not owing to dominant-negative effect, but rather owing to mutp53 GOF activities. Thus, we performed a search for functional annotations within this list. The most significant enrichment of 15 genes was for 'multicellular organismal development' with a P -value of 7.4×10^{-5} (see Supplementary Table S4).

Isolation of total RNA. Total RNA for QRT-PCR was isolated using NucleoSpin RNA extract kit (Macherey-Nagel, Duren, Germany) according to the manufacturer's protocol.

Quantitative real-time PCR. A 2 μ g aliquot of the total RNA was reverse transcribed using MMLV RT (Promega, Madison, WI, USA) and random hexamer primers. QRT-PCR was performed using SYBR Green PCR Master Mix (Applied Biosystems) on an ABI 7300 instrument (Applied Biosystems, Singapore). The expression level for each gene was normalized to that of the *GAPDH* housekeeping gene in the same sample. The primers were designed using the Primer Express software.

Three-dimensional cell culture. EP156T-derived cells were seeded on eight-well Lab Tek chamber slides (Nalgene Nunc International, Rochester, NY, USA) coated with Matrigel (BD Biosciences, San Jose, CA, USA) in MCDB-153 + medium with 2% Matrigel. The medium was replaced every 4 days. Spheroid structures were analyzed following 10 days of incubation and photographs were taken.

Invasion assay. For trans-well invasion assays, 1.5×10^5 cells in serum-free medium were added to the top chambers of 24-well trans-well plates (8 μ m size; Cell Biolabs Inc., San Diego, CA, USA), which were coated with Matrigel (BD Biosciences) diluted 1:5 in serum-free media. Media containing 10% fetal calf serum were added to the bottom chambers. Plates were incubated in 37°C for 24 h, and then cells at the bottom (invading) were stained and absorbance was recorded according to the manufacturer's instructions.

ChIP analysis. ChIP was conducted as described in Weisz *et al.*²⁸ Briefly, sonicated chromatin prepared from 1 to 5×10^6 cells was immunoprecipitated using the CHIPAb + trimethyl-histone H3 (Lys27) (Cat. no. 17–622; Upstate, Waltham, MA, USA) antibody. The enrichment of specific DNA sequences was measured by QRT-PCR.

Immunofluorescent staining. EP156T cells seeded on glass coverslips were incubated for 48 h. Slides were then fixed in 4% paraformaldehyde in PBS for 10 min, rinsed $3 \times$ with PBS, blocked for 30 min with PBS containing 0.1% Triton X-100, 5% goat serum and 0.2% bovine serum albumin, and incubated for 1 h with either anti-E-cadherin (generously provided by Dr. R. Berger, Tel Hashomer, Israel) or with anti-fibronectin (a generous gift from Dr. B. Geiger, The Weizmann Institute, Rehovot, Israel). Slides were washed $3 \times$ with PBS, incubated with secondary antibodies conjugated to Alexa 466 (Molecular Probes, Eugene, OR, USA) or Cy3 (Chemicon, Temecula, CA, USA) for 1 h together with DAPI, and visualized under a fluorescence microscope.

Conflict of interest

The authors declare no conflict of interest.

Acknowledgements. This research was supported by a Center of Excellence grant from Flight Attendant Medical Research Institute (FAMRI), EC FP6 Grant LSHC-CT-2004-503576, the Yad Abraham Center for Cancer Diagnosis and Therapy and the Ridgefield Foundation. Partial funding was provided by the Center for Women's Health Research. This publication reflects the authors' views and not necessarily those of the European Community. The EC is not liable for any use that may be made of the information contained herein. VR is the incumbent of the Norman and Helen Asher Professorial Chair Cancer Research at the Weizmann institute. ED is the incumbent of the Henry J Leir Professorial Chair. We are grateful to Alla Voldman and Leslie Pomeranic for technical assistance.

- Fridman JS, Lowe SW. Control of apoptosis by p53. *Oncogene* 2003; **22**: 9030–9040.
- Vousden KH. p53: death star. *Cell* 2000; **103**: 691–694.
- Bullock AN, Fersht AR. Rescuing the function of mutant p53. *Nat Rev Cancer* 2001; **1**: 68–76.
- Sigal A, Rotter V. Oncogenic mutations of the p53 tumor suppressor: the demons of the guardian of the genome. *Cancer Res* 2000; **60**: 6788–6793.
- Cadwell C, Zambetti GP. The effects of wild-type p53 tumor suppressor activity and mutant p53 gain-of-function on cell growth. *Gene* 2001; **277**: 15–30.
- Weisz L, Oren M, Rotter V. Transcription regulation by mutant p53. *Oncogene* 2007; **26**: 2202–2211.
- Heidenberg HB, Bauer JJ, McLeod DG, Moul JW, Srivastava S. The role of the p53 tumor suppressor gene in prostate cancer: a possible biomarker? *Urology* 1996; **48**: 971–979.
- Zeng L, Rowland RG, Lele SM, Kyprianou N. Apoptosis incidence and protein expression of p53, TGF-beta receptor II, p27Kip1, and Smad4 in benign, premalignant, and malignant human prostate. *Hum Pathol* 2004; **35**: 290–297.
- Kogan I, Goldfinger N, Milyavsky M, Cohen M, Shats I, Dobler G *et al.* hTERT-immortalized prostate epithelial and stromal-derived cells: an authentic *in vitro* model for differentiation and carcinogenesis. *Cancer Res* 2006; **66**: 3531–3540.
- Shi XB, Nesslering NJ, Deitch AD, Gumerlock PH, deVere White RW. Complex functions of mutant p53 alleles from human prostate cancer. *Prostate* 2002; **51**: 59–72.
- Milyavsky M, Shats I, Erez N, Tang X, Senderovich S, Meerson A *et al.* Prolonged culture of telomerase-immortalized human fibroblasts leads to a premalignant phenotype. *Cancer Res* 2003; **63**: 7147–7157.
- Yang J, Mani SA, Donaher JL, Ramaswamy S, Itzykson RA, Come C *et al.* Twist, a master regulator of morphogenesis, plays an essential role in tumor metastasis. *Cell* 2004; **117**: 927–939.
- Kwok WK, Ling MT, Lee TW, Lau TC, Zhou C, Zhang X *et al.* Up-regulation of TWIST in prostate cancer and its implication as a therapeutic target. *Cancer Res* 2005; **65**: 5153–5162.
- Wallerand H, Robert G, Pasticier G, Ravaud A, Ballanger P, Reiter RE *et al.* The epithelial-mesenchymal transition-inducing factor TWIST is an attractive target in advanced and/or metastatic bladder and prostate cancer(s). *Urol Oncol* 2009, in press (e-pub ahead of print 9 March 2009).
- Debnath J, Muthuswamy SK, Brugge JS. Morphogenesis and oncogenesis of MCF-10A mammary epithelial acini grown in three-dimensional basement membrane cultures. *Methods* 2003; **30**: 256–268.
- Debnath J, Brugge JS. Modelling glandular epithelial cancers in three-dimensional cultures. *Nat Rev Cancer* 2005; **5**: 675–688.
- Feinberg AP. Phenotypic plasticity and the epigenetics of human disease. *Nature* 2007; **447**: 433–440.
- Bernstein BE, Meissner A, Lander ES. The mammalian epigenome. *Cell* 2007; **128**: 669–681.

19. Lang GA, Iwakuma T, Suh YA, Liu G, Rao VA, Parant JM *et al*. Gain of function of a p53 hot spot mutation in a mouse model of Li–Fraumeni syndrome. *Cell* 2004; **119**: 861–872.
20. Gaiddon C, Lokshin M, Ahn J, Zhang T, Prives C. A subset of tumor-derived mutant forms of p53 down-regulate p63 and p73 through a direct interaction with the p53 core domain. *Mol Cell Biol* 2001; **21**: 1874–1887.
21. Crum CP, McKeon FD. p63 in epithelial survival, germ cell surveillance, and neoplasia. *Annu Rev Pathol* 2010; **5**: 349–371.
22. van Oijen MG, Slootweg PJ. Gain-of-function mutations in the tumor suppressor gene p53. *Clin Cancer Res* 2000; **6**: 2138–2145.
23. Di Agostino S, Strano S, Emiliozzi V, Zerbini V, Mottolese M, Sacchi A *et al*. Gain of function of mutant p53: the mutant p53/NF-Y protein complex reveals an aberrant transcriptional mechanism of cell cycle regulation. *Cancer Cell* 2006; **10**: 191–202.
24. Choi YJ, Choi YL, Cho EY, Shin YK, Sung KW, Hwang YK *et al*. Expression of Bmi-1 protein in tumor tissues is associated with favorable prognosis in breast cancer patients. *Breast Cancer Res Treat* 2009; **113**: 83–93.
25. Pietersen AM, Horlings HM, Hauptmann M, Langerød A, Ajouaou A, Cornelissen-Steijger P *et al*. EZH2 and BMI1 inversely correlate with prognosis and TP53 mutation in breast cancer. *Breast Cancer Res* 2008; **10**: R109.
26. Ashburner M, Ball CA, Blake JA, Botstein D, Butler H, Cherry JM *et al*. Gene ontology: tool for the unification of biology. The gene ontology consortium. *Nat Genet* 2000; **25**: 25–29.
27. Dennis Jr G, Sherman BT, Hosack DA, Yang J, Gao W, Lane HC *et al*. DAVID: Database for Annotation, Visualization, and Integrated Discovery. *Genome Biol* 2003; **4**: P3.
28. Weisz L, Zalcenstein A, Stambolsky P, Cohen Y, Goldfinger N, Oren M *et al*. Transactivation of the EGR1 gene contributes to mutant p53 gain of function. *Cancer Res* 2004; **64**: 8318–8327.

Supplementary Information accompanies the paper on Cell Death and Differentiation website (<http://www.nature.com/cdd>)